STRUCTURAL AND BINDING ANALYSIS OF A TWO DOMAIN EXTRACELLULAR CD2 MOLECULE

By PETER H. SAYRE, REBECCA E. HUSSEY, HSIU-CHING CHANG, THOMAS L. CIARDELLI, and ELLIS L. REINHERZ

From the Laboratory of Immunobiology, Dana-Farber Cancer Institute and Departments of Pathology and Medicine, Harvard Medical School, Boston, Massachusetts 02115; and Department of Pharmacology and Toxicology, Dartmouth Medical School, Hanover, New Hampshire 03756

The human CD2 (T11) molecule is a 50-kD surface glycoprotein expressed on >95% of thymocytes and virtually all peripheral T lymphocytes that mediates both adhesion between these cells and their cognate partners, as well as subsequent activation events. Specific combinations of antibodies against the surface-bound molecule can activate IL-2-dependent T cell proliferation, helper T cell function, and cytotoxicity by NK cells and CTL (1–3) in the absence of cellular adhesion. In addition, thymocyte activation can be mediated via CD2 (4, 5). The role of CD2 in approximation of T cells to various cell types, including human thymic epithelial cells, B cells, target cells, and sheep erythrocytes has been demonstrated to depend on direct interaction between CD2 and the broadly distributed human LFA-3 surface glycoprotein or its sheep homologue, T11TS (5–10).

Biochemical analyses using specific mAbs show that CD2 is T lineage specific and exists on the cell surface in several differentially glycosylated forms (11–13). CD2 cDNA clones predict a cleaved signal peptide of 24 amino acid residues, an extracellular segment of 185 residues, a transmembrane domain of 25 residues, and a cytoplasmic region of 117 residues (13–16). The corresponding genomic organization reveals a single exon encoding the signal peptide (less four residues), two exons encoding the extracellular segment, one exon encoding the transmembrane domain and charged membrane anchor segment, and one exon encoding the cytoplasmic region (17).

A prerequisite for in-depth structure-function analysis of cell surface receptors is the capacity to produce and analyze sufficient quantities of material that bear a high degree of fidelity to the native structure. Preliminary observations suggested that a baculovirus expression system could provide such a capability. However, due to the nature of the cDNA construction, monomeric CD2 was not obtained. Here we report the production and characterization of a recombinant soluble CD2 molecule, termed $T11_{ex2}$, that corresponds to the two extracellular segment exons and exists in solution entirely in monomeric form. The folding of the recombinant CD2 protein appears to be native since it reacts with mAbs that were produced against transmembrane CD2 on the surface of human T lymphocytes. Surprisingly, the affinity of the CD2 extracellular segment monomer is only micromolar, implying that the avidity of CD2-mediated T cell adhesion is dependent on cooperative binding resulting from the multiple copies of CD2 on the T lymphocyte surface. To our knowledge, this represents the first time that a lymphoid adhesion receptor has been produced on a milligram scale in a functional and pure form.

J. Exp. Med. © The Rockefeller University Press · 0022-1007/89/03/995/15 $2.00
Volume 169 March 1989 995–1009

Materials and Methods

Baculovirus Transfer Vector Plasmid Construct for $T11_{ex2}$. The plasmid pAc373/$T11_{ex2}$ was constructed by digestion of pGEM-4-S1, a pGEM derivative containing a 950-bp fragment of the CD2 cDNA PB2 (13) with Pvu II, which digests the cDNA at nucleotide position 628 near the start of the transmembrane region. A double-stranded synthetic oligonucleotide linker:

CTGTCCAGAGAAATAAGGATCCT
GACAGGTCTCTTTATTCCTAGGA

containing the last base for the Ser-178 codon, codons for Cys-Pro-Glu-Lys, a stop codon, and a Bam HI restriction site was synthesized and ligated to the blunt Pvu II ends. After Bam HI digestion, the insert was cloned into the Bam HI site of the pAc373 baculovirus transfer vector (18). All restriction enzymes were purchased from New England Biolabs (Beverly, MA).

Recombinant Protein Production. Transfer of the $T11_{ex2}$ sequences from the plasmid vector to the AcNPV genome to generate recombinant baculovirus $T11_{ex2}$-AcNPV was accomplished essentially as described (18, 19). Metabolic labeling with [^{35}S]cysteine of $T11_{ex2}$-AcNPV-infected SF9 cells was carried out as described (19). Metabolically labeled culture supernatants were harvested, microfuged for 10 min and subjected to immunoprecipitation for 16 h at 4°C with a monoclonal anti-CD2 antibody (anti-$T11_1$, 3T4-8B5) linked to Affigel-10 (Bio-Rad Laboratories, Richmond, CA) beads (10 mg mAb/ml gel). After immunoabsorption the beads were washed twice with lysis buffer and bound material eluted with 0.1 M glycine, HCl buffer, pH 2. Eluates were analyzed by SDS-PAGE in 12.5% gels. Large protein production was performed as described (19), except that proteins were purified over an anti-$T11_1$ (3T4-8B5) immunoaffinity column.

Protein Microsequencing. Proteins were prepared for microsequencing by electrophoresis on 12.5% polyacrylamide gels, followed by electroblotting onto polyvinylidene difluoride membranes according to the method of Matsudaira (20). After visualization with Coomassie blue, stained bands were excised and loaded onto a sequencer (No. 470; Applied Biosystems, Inc., Foster City, CA) and sequenced using the 03RPTH program.

Endoglycosidase F Digestion of $T11_{ex2}$. 1 μg samples of purified $T11_{ex2}$ dialyzed against PBS were incubated in Endo-F buffer (0.1 M sodium phosphate, 1% NP-40, 1% 2-ME, 50 mM EDTA, 1 mM PMSF, pH 6.1) in the presence of 0.7 U Endo-F (New England Nuclear, Boston, MA) in 7 μl reaction volumes. Digestion was arrested at the indicated times by addition of 15 μl SDS sample buffer, boiling for 5 min and freezing at −20°C before analysis by 12.5% SDS-PAGE.

Equilibrium Sedimentation. Sedimentation studies were performed by using the short column, high speed meniscus-depletion method of Yphantis (21) and Richardson et al. (22). Standard double-sector cells, equipped with sapphire windows, 4-mm solution column lengths, and a temperature of 21°C were used.

Papain Digestion. 32 ng papain was added to 8 μg samples of $T11_{ex2}$ at 0.5 μg/ml in PBS containing 10 mM DTT for an enzyme/protein ratio of 1:250. Samples were incubated at 37°C for 15, 30, 45, or 60 min. Digestions were stopped by the addition of SDS sample buffer and boiling for 5 min. Samples were electrophoresed on a 12.5% polyacrylamide gel and stained with Coomassie blue.

Circular Dichroism. Far ultraviolet CD spectra were obtained on an Instruments S.A., Inc., (Metuchen, NJ) Jobin Yvon circular dichrograph calibrated with (+)10-camphorsulfonic acid and epiandosterone. Measurements were taken at 25, 50, and 80°C ± 0.1°C in 10 mM sodium phosphate, pH 7.2, in a 1-mm cell. All spectra represent an average of three to five individual spectra with data taken at 0.5-mm intervals using a 10-s response time for each point. Protein concentrations were determined by quantitative amino acid analysis of aliquots taken from the sample cells.

Rosette Inhibition Assay. Jurkat cells were washed in supplemental MEM (SMEM)/2% FCS (wash) and resuspended at 10^7/ml. Sheep erythrocytes were washed twice in HBSS and resuspended in wash to 5% vol/vol. 10 μl of sheep erythrocytes were aliquoted into 12-75-mm plastic tubes and 100 μl wash, $T11_{ex2}$ protein or control soluble CD4 $T4_{ex1}$ protein (19) was

added, followed by incubation at 4°C for 30 min. Subsequently, 20 μl of Jurkat cells were added, and after 5 min they were centrifuged at 800 rpm in a Sorvall RT6000, followed by incubation at 4°C for 1 h. The cell mixture was gently resuspended and mounted on glass slides with cover slips and rosette formation was assessed on a Zeiss photomicroscope.

Radiolabeled $T11_{ex2}$ Binding Assays. The purified recombinant soluble CD2 external domain molecule $T11_{ex2}$ was radioiodinated as follows: 50 μl $T11_{ex2}$ (1 mg/ml) dialyzed against PBS was labeled with 10 μl of immobilized lactoperoxidase/glucose oxidase (Enzymobeads; Bio-Rad Laboratories) in 40 mM sodium phosphate, pH 7.2, 0.4% glucose, and 1 mCi ^{125}I for 5 min. After quenching the reaction for 20 min with 20 mM sodium iodide and 0.02% sodium azide, 20 μl FCS was added and the free iodine was separated on a 1-ml Bio-Gel P-6 column (Bio-Rad Laboratories) conditioned with 0.2M sodium phosphate, pH 7.2, and 10% FCS and run in the same buffer.

Cold Competition Studies. 5×10^6 cpm radiolabeled $T11_{ex2}$ (2.8×10^8 cpm/nmol) was added at 0.1 μM to 1.8×10^6 JY cells overlayed onto 0.2 ml of a 1.5:1 mixture of dibutyl phthalate:dioctyl phthalate (Aldrich Chemical Co., Milwaukee, WI) in 0.5-ml plastic tubes as described in Teshigawara et al. (23). Increasing concentrations of unlabeled $T11_{ex2}$ or $T4_{ex1}$ were added in a final volume of 200 μl in RPMI 1640/10% FCS. After a 1-h incubation at 4°C, the tubes were centrifuged (8,500 *g* for 1 min), the tips of the tubes containing the cell pellets were cut, and the cell-bound and free radioactivity were determined in a gamma counter. To some tubes, anti-LFA-3 antibody TS2/9 (generously provided by Dr. Timothy Springer, Dana Farber Cancer Institute, Boston, MA) was added at 50 μg/ml as a separate determination of nonspecific binding. This concentration of anti-LFA-3 was independently shown to give maximal inhibition of $T11_{ex2}$ binding. Specific activity was calculated using a molecular weight for $T11_{ex2}$ of 30,000. Protein concentrations were determined by quantitative amino acid analysis of standard $T11_{ex2}$ samples. Subsequent samples were compared with standards by Coomassie blue staining of twofold dilutions of standard and test samples run on the same gel and analyzed by densitometry.

Saturation Binding Studies. Increasing concentrations of radiolabeled $T11_{ex2}$ (1.31×10^7 cpm/nmol) were added to 2.6×10^6 JY cells in the presence or absence of 50 μg/ml anti-LFA-3 antibody to determine nonspecific binding. Binding was carried out as above and the dissociation constant was determined by Scatchard analysis after subtraction of nonspecific binding determined in the presence of anti-LFA-3.

Results

Production and Purification of $T11_{ex2}$. We designed a construct for expression of a soluble fragment of CD2 that would include all the residues encoded by the leader and two extracellular segment exons (Fig. 1, exons 1–3). The plasmid pAc373/$T11_{ex2}$ was constructed as described in Materials and Methods and encodes 182 amino acids of the predicted CD2 external segment including all the residues derived from the

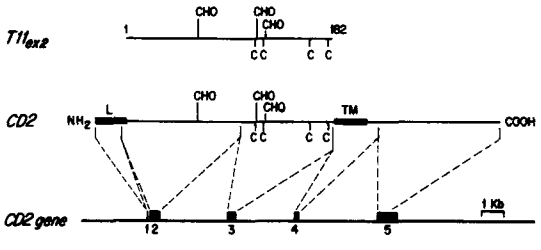

FIGURE 1. Structure of recombinant soluble $T11_{ex2}$, native CD2, and its genomic organization. A schematic of the 182 extracellular CD2 amino acids comprising $T11_{ex2}$ (*top*) is compared with CD2 protein structure (*middle*). The positions of cysteine residues (C), N-linked carbohydrate addition sites (CHO), the CD2 leader segment (L), and the CD2 transmembrane domain (TM) are indicated. In the CD2 gene (*bottom*), exon 1 corresponds to CD2 amino acid residues −24 to −4, exon 2 to residues −4 to 103, exon 3 to residues 104 to 180, exon 4 to residues 181 to 221, and exon 5 to residues 222 to 327 (17).

two extracellular exons (Fig. 1) and part of one codon (for Glu-181) and all of a second codon (for Lys-182) derived from the transmembrane domain exon. This construction thus includes all four extracellular cysteine residues located in domain II of CD2 and thereby avoids problems associated with intermolecular disulfide exchange observed with a previous construction (24).

Plasmid pAc373/T11$_{ex2}$ was used to co-transfect SF9 cells with AcNPV baculoviral DNA. Recombinant baculovirus, termed T11$_{ex2}$-AcNPV, were selected, purified, and used to infect small-scale cultures for metabolic labeling. Immunoprecipitation of radiolabeled supernatants with anti-T11$_1$ (3T4-8B5), an anti-CD2-specific mAb (1), verified that T11$_{ex2}$-AcNPV directed the production of a recombinant CD2 molecule in SF9 cells (data not shown). T11$_{ex2}$-AcNPV was therefore used to infect liter cultures for the production of large amounts of protein. T11$_{ex2}$ protein was purified from infected cell supernatants by affinity chromatography on an anti-T11$_1$ column.

Biochemical Characterization of T11$_{ex2}$. T11$_{ex2}$ migrates as a well-demarcated doublet in both reducing and nonreducing conditions in SDS-PAGE (Fig. 2, lanes *a* and *b*). Two well-separated bands at 30–31 kD are seen in the presence of 50 mM of DTT (lane *a*), which migrate at 27–28 kD in the absence of reducing agent (lane *b*). The clear-cut decrease in electrophoretic mobility after reduction with DTT strongly indicates that T11$_{ex2}$ contains intrachain disulfide bridges; it does not form interchain bridges. Although not shown, microsequencing analysis of [^{35}S]cysteine-labeled peptides verifies that there are two sets of intrachain disulfide bonds in T11$_{ex2}$ between the NH_2-terminal cysteines and COOH-terminal cysteines.

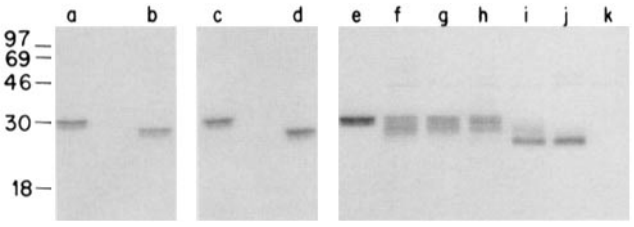

FIGURE 2. Purification, radioiodination, and endoglycosidase digestion of T11$_{ex2}$. Lanes *a–d*: 1 μg T11$_{ex2}$ purified from large scale cultures of SF9 cells infected with T11$_{ex2}$-AcNPV was analyzed by Coomassie staining on a 12.5% polyacrylamide gel in the presence of 50 mM DTT (lane *a*) or in nonreducing conditions (lane *b*). An aliquot of T11$_{ex2}$ radioiodinated with solid-phase lactoperoxidase/glucose oxidase was analyzed on the same gel in the presence (lane *c*) or absence (lane *d*) of 50 mM DTT by autoradiography. Lanes *e–k*: 1 μg purified T11$_{ex2}$ was digested with 0.7 U Endo-F for varying amounts of time and the reaction was stopped by the addition of SDS sample buffer before SDS-PAGE analysis and Coomassie staining. (Lane *e*) No enzyme; (lane *f*) simultaneous addition of enzyme and sample buffer; (lanes *g–j*) 1 min, 5 min, 1 h, 18 h digestion ; (lane *k*) 0.7 U Endo-F alone.

To investigate the difference between the two bands representing $T11_{ex2}$, 160 pmol of purified protein was separated by SDS-PAGE and blotted onto a polyvinyl difluoride (PVDF) membrane (20). The upper and lower bands were cut separately from the membrane for NH_2-terminal sequencing. Each band yielded the CD2 NH_2-terminal sequence, suggesting that they differ from one another by posttranslational modification. As shown in Fig. 2, endoglycosidase digestion generates at least five distinct bands. After short digestion times, two new lower molecular weight species are generated (lanes *f–h*). Some glycans on $T11_{ex2}$ are apparently quite susceptible to digestion since even after simultaneous addition of enzyme and SDS sample buffer, these new species are generated (lane *f*). After 1 h digestion, most of the $T11_{ex2}$ protein is digested to a 25-kD species (lane *i*); overnight digestion results in complete digestion to a single band at 25-kD (lane *j*). Note that the band of approximately 45-kD size represents the Endo-F enzyme since it appears in lane *k*, where an equivalent amount of enzyme alone has been analyzed. The origin of the faint band at 48-kD in lane *j* is unclear.

To determine whether $T11_{ex2}$ exists as a noncovalently linked multimer in aqueous solution, it was subjected to equilibrium sedimentation by the high-speed meniscus depletion method (21) in both aqueous and dissociating conditions. As shown in Fig. 3, the calculated molecular weights for both conditions are very similar (25.3 kD in aqueous solution vs. 24.7 kD in dissociating conditions). This result demonstrates that $T11_{ex2}$ exists as a monomer in solution.

The expression of CD2 epitopes was investigated by immunoprecipitation analysis. The $T11_{ex2}$ molecule can be immunoprecipitated by both anti-$T11_1$ and a second mAb to a different epitope termed anti-$T11_2$. However, $T11_{ex2}$ is not immunoprecipitated by the anti-CD2 antibody anti-$T11_3$, which defines an activation specific epitope on CD2. Nevertheless, $T11_{ex2}$ was able to inhibit the binding of anti-$T11_3$-FITC to the $T11_3^+$ Jurkat cell line at a concentration of 10 μM, implying its presence on $T11_{ex2}$ (data not shown). These results also suggest that the affinity of anti-$T11_3$ for its epitope is low.

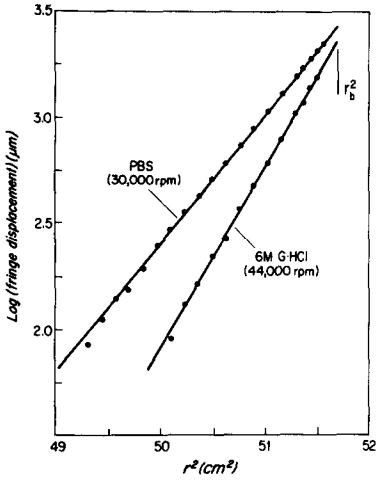

FIGURE 3. Equilibrium sedimentation analysis. Plots of log (fringe displacement) against square of distance from center of rotation, r^2. $T11_{ex2}$ (0.05%) was analyzed by sedimentation equilibrium on an analytical ultracentrifuge (model E; Beckman Instruments, Fullerton, CA) in aqueous solution (PBS) at 30,000 rpm ($\omega = 3.142 \times 10^3$ rad/s) or in dissociating conditions (6 M guanidine hydrochloride) at 44,000 rpm ($\omega = 4.608 \times 10^3$ rad/s). Data were obtained at 22°C (PBS) or 23°C (guanidine-hydrochloride). Assuming a partial specific volume of 0.725, the calculated molecular weight from the displayed slope and using the equation: molecular weight = 4.606 RT slope/$[\omega^2 (1 - \bar{v}\omega)]$ is 225,315 in aqueous solution. Assuming a partial specific volume (denoted as $\bar{v}$) of 0.725 - 0.1 in 6 M guanidine-hydrochloride (22), the calculated molecular weight is 24,736 in dissociating conditions.

Secondary structure predictions suggest the presence of both α-helical and β-sheet structure in the CD2 external domain (16). To more directly predict secondary structural characteristics, the $T11_{ex2}$ molecule was evaluated by circular dichroism. As shown in Fig. 4 *A*, the far ultraviolet CD spectrum of $T11_{ex2}$ in 10 mM of sodium phosphate shows a positive absorption maximum at about 200 nm ($\Delta\epsilon$ = 0.459), a negative minimum at 215 nm ($\Delta\epsilon$ = −1.94), and a shoulder at 225 nm ($\Delta\epsilon$ = −1.0). When the $T11_{ex2}$ molecule is reduced by 50 mM DTT and subsequently alkylated with iodoacetamide, the CD spectrum is substantially altered, pointing to a role for disulfide bridges in stabilizing secondary and tertiary structure (Fig. 4 *B*). The fact that the spectrum of the nonreduced molecule reflects significant thermal denaturation at 80°C (Fig. 4 *C*) confirms that substantial secondary structure is present in soluble $T11_{ex2}$. As expected, the pattern after thermal denaturation is the same for the reduced as for the nonreduced molecule (compare Fig. 4, *C* and *D*).

In its overall pattern, the CD spectrum resembles that for Thy-1 (25), which is a well-recognized member of the Ig superfamily (26) and is therefore predicted to consist entirely of β-sheet. However, the shoulder at 225 nm is absent from the Thy-1 profile. To obtain a more objective prediction of secondary structure from the CD spectrum, the digitalized absorption data (Table I) were deconvoluted according to the inverse matrix method of Compton and Johnson (27). The resulting predictions for proportions of secondary elements are: α-helix, 20%; antiparallel β-sheet, 13%; parallel β-sheet, 9%; turn, 20%; other, 46%. Since none of the proteins in the data set used to determine the matrix values are homologous to CD2, the predicted frac-

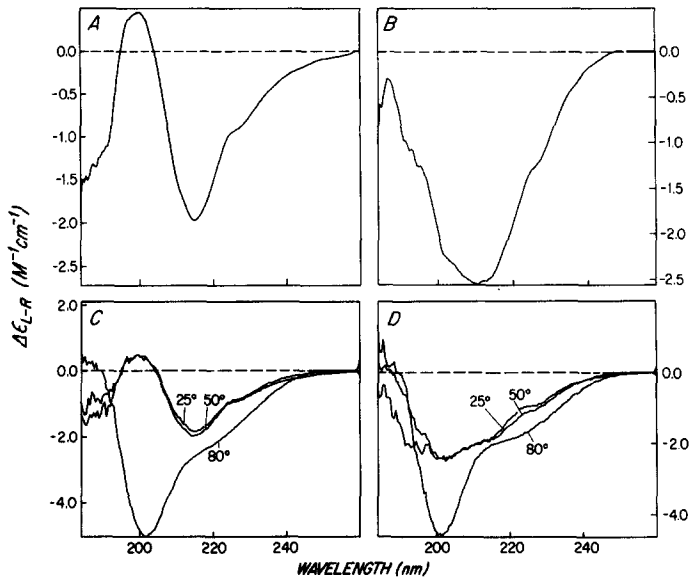

FIGURE 4. Circular dichroism spectra of $T11_{ex2}$. Far ultraviolet circular dichroism spectra represent the average of three to five individual spectra with data taken at 0.5 nm wavelength intervals in 10 mM sodium phosphate, pH 7.2. (*A*) Spectrum at 25°C of untreated $T11_{ex2}$; (*B*) spectrum of $T11_{ex2}$ reduced with 10 μM DTT and alkylated with 20 μM iodoacetamide; (*C*) thermal denaturation of the sample in *A*; (*D*) thermal denaturation of the sample in *B*.

TABLE I
Digitized Protein Circular Dichroism Spectrum for $T11_{ex2}$ from 184–260 nm at 2-nm Intervals

Wavelength	Δε	Wavelength	Δε
184	−1.49	224	−1.002
186	−1.50	226	−0.923
188	−1.345	228	−0.856
190	−1.176	230	−0.743
192	−1.026	232	−0.629
194	−0.284	234	−0.515
196	0.241	236	−0.426
198	0.411	238	−0.348
200	0.459	240	−0.282
202	0.360	242	−0.234
204	0.027	244	−0.195
206	−0.432	246	−0.151
208	−0.959	248	−0.112
210	−1.467	250	−0.089
212	−1.750	252	−0.077
214	−1.949	254	−0.062
216	−1.930	256	−0.044
218	−1.771	258	−0.018
220	−1.515	260	−0.018
222	−1.241		

Spectrum was taken in 10 mM sodium phosphate (pH 7.2) in a 1-mm cell at 22°C. Secondary structure predictions were calculated by taking dot products with inverse CD spectra for the five secondary structure categories as described previously (27); see Table VI. The calculated results are: α-helix, 20%; antiparallel β-sheet, 13%; parallel β-sheet, 9%; turn, 20%; other, 46%. Units for Δε are M^{-1}/cm^{-1}.

tions of secondary structure are only approximate. When the same CD data are deconvoluted by the method of Yang et al. (28), 15% α and 40% β structures are predicted.

To investigate the presence of protease-resistant domains in the $T11_{ex2}$ molecule, limited papain digestions were performed. 15 min of digestion at an enzyme/protein ratio of 1:250 at 37°C yields a major band at 15 kD when analyzed by SDS-PAGE (data not shown). Longer digestion times cause partial disappearance of the 15-kD band. Approximately 400 pmol of this 15-kD material was blotted onto PVDF and sequenced, yielding 19 unambiguous residues corresponding to the CD2 NH_2 terminus. These results demonstrate that the COOH region of $T11_{ex2}$ is much less resistant to papain digestion that its NH_2-terminal counterpart.

$T11_{ex2}$ Inhibits Sheep Erythrocyte Rosetting. We next tested the ability of $T11_{ex2}$ to interact with the CD2 ligand expressed on the surface of various cell types. The capacity of $T11_{ex2}$ to inhibit sheep erythrocyte rosetting with T lymphocytes was tested. Table II shows that rosetting is completely inhibited at concentrations of $T11_{ex2}$ >5 μM; half-maximal inhibition occurs between 0.63 and 1.25 μM $T11_{ex2}$. Note that the anti-$T11_1$ (3T4-8B5) antibody abrogates rosetting at a concentration as low as 0.007 μM (Table II). This results suggests that any direct interaction between the soluble $T11_{ex2}$ molecule and the CD2 ligand is of relatively low affinity.

TABLE II

Concentration Dependence of $T11_{ex2}$ Inhibition of Sheep Erythrocyte–Human T Cell Rosettes

Protein added	Amount	Rosettes (percent of control)
	μM	
None		100
$T11_{ex2}$	20	0
	10	0
	5	0
	2.5	4.8
	1.25	9.9
	0.63	122
	0.31	84
	0.16	116
	0.08	110
$T4_{ex1}$	20	66
	10	91
	5	96
	2.5	105
	1.25	90
	0.63	72
	0.31	110
	0.16	99
	0.08	116
Anti-CD2	0.7	0
	0.07	0
	0.007	0

For rosette formation, sheep erythrocytes were preincubated with soluble protein or antibody at the indicated concentrations for 1 h at 4°C followed by the addition of Jurkat cells, cocentrifugation, and a further 1-h incubation at 4°C. Rosettes were counted in a hemacytometer. Control value was the fraction of rosette formation in the absence of added protein. Anti-CD2 was the anti-$T11_1$ antibody 3T4-8B5.

$T11_{ex2}$ Blocks the Binding of Anti-LFA-3 mAb. To investigate whether $T11_{ex2}$ could interact with a previously defined ligand for CD2 on human cells (9), its ability to block the binding of anti-LFA-3 mAb TS9/2 (29) to LFA-3-bearing cells was tested. Specifically, anti-LFA-3 reactivity was measured by FACS analysis on the human B-lymphoblastoid line JY, which expresses high levels of LFA-3. As shown in Table III, preincubation of JY cells with soluble CD4 does not affect this staining, whereas preincubation with 10 μM $T11_{ex2}$ causes a substantial decrease in observed fluorescence, reducing linear immunofluorescence from channel 120 to 30.6. This represents a reduction of 85% of specific anti-LFA-3 reactivity (calculated after subtraction of the background fluorescence of 13.2 linear units). Significant blocking is also seen at 1 μM but not at 0.1 μM. Addition of the control soluble CD4 $T4_{ex1}$ protein has no effect on anti-LFA-3 binding. Thus, by this measure as well as by inhibition of sheep erythrocyte rosetting, the affinity of $T11_{ex2}$ for its ligand is apparently in the micromolar range.

TABLE III
Concentration Dependence of $T11_{ex2}$ Inhibition of Anti-LFA-3 Antibody Binding

Protein added	Amount		Anti-LFA-3 antibody added	Mean fluorescence intensity
	μg/ml	*(μM)*		
$T11_{ex2}$:	300	(10)	+	30.6
	30	(1)	+	66.1
	3	(0.1)	+	109.1
	0.3	(0.01)	+	119.8
$T4_{ex1}$:	300		+	125.1
	30		+	120.2
	3		+	117.6
	0.3		+	116.9
None			+	123.7
			–	13.2

Mean fluorescence intensities were obtained on a linear scale from 0 to 250.

$T11_{ex2}$ Binds to LFA-3 on Human B Lymphoblastoid Cells. Since $T11_{ex2}$ clearly inhibits sheep erythrocyte rosetting and blocks the binding of anti-LFA-3 antibody, we determined whether specific, saturable binding of $T11_{ex2}$ to human cells bearing LFA-3 could be detected. Two types of binding assays were used. In the first, increasing amounts of unlabeled $T11_{ex2}$ was added to a mixture of the JY B-lymphoblastoid cell line plus a constant amount of ^{125}I-labeled $T11_{ex2}$ (ligand). As shown in Fig. 5, binding of radiolabeled $T11_{ex2}$ is progressively inhibited by the addition of increasing amounts of unlabeled molecules. Half-maximal inhibition occurs at ~0.5 μM of $T11_{ex2}$. In contrast and as expected, addition of soluble CD4 $T4_{ex1}$ protein has no effect on ^{125}I-labeled $T11_{ex2}$ binding to JY.

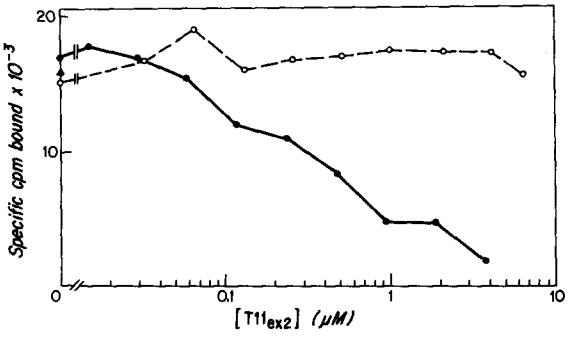

FIGURE 5. Competitive inhibition of radioiodinated $T11_{ex2}$ binding to JY cells. 5×10^6 cpm radiolabeled $T11_{ex2}$ (2.8×10^8 cpm/nmol) was added at 0.1 μM to 1.8×10^6 JY cells overlayed onto 0.2 ml of a 1.5:1 mixture of dibutyl phthalate/dioctyl phthalate in 0.5-ml plastic tubes. Increasing concentrations of unlabeled $T11_{ex2}$ (*closed circles*) or $T4_{ex1}$ as a control (*open circles*) were added in a final volume of 200 μl in RPMI 1640/10% FCS. After a 1-h incubation at 4°C, tubes were spun, cell pellets were severed, and bound radioactivity was determined. To one tube anti-LFA-3 antibody TS2/9 was added at 50 μg/ml as a determination of nonspecific binding. Specific cpm are the total cpm minus cpm bound in the presence of anti-LFA-3 (9,070 cpm). Binding in the presence of control anti-HLA mAb W6/32 is also shown (*triangle*).

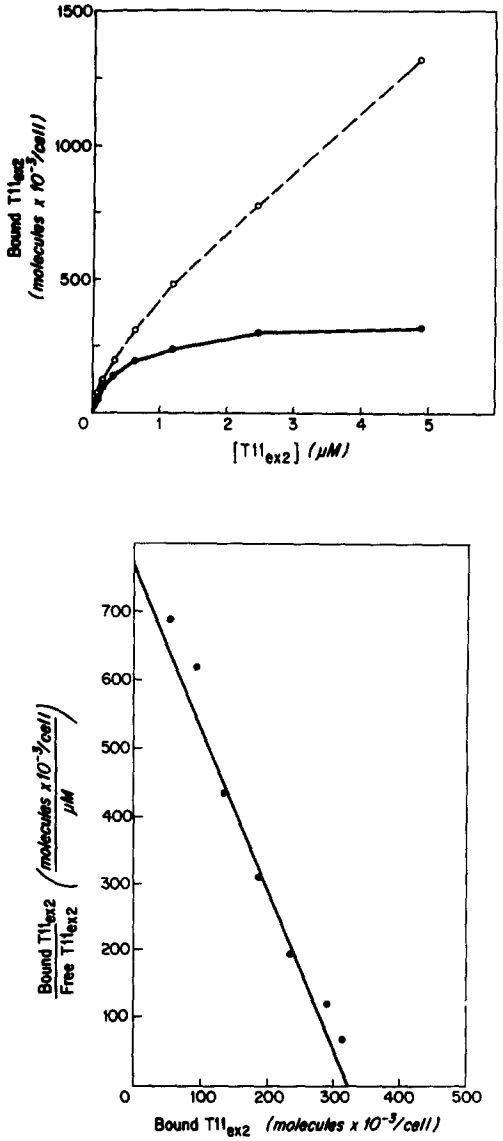

FIGURE 6. Saturation binding of $T11_{ex2}$ to JY cells and Scatchard analysis. Increasing concentrations of radiolabeled $T11_{ex2}$ (1.31×10^7 cpm/nmol) were added to 2.6×10^6 JY cells in the presence or absence of 50 μg/ml anti-LFA-3 antibody to determine nonspecific binding. Binding was carried out as above and the dissociation constant was determined by Scatchard analysis after subtraction of nonspecific binding determined in the presence of anti-LFA-3. (*Top*) Total binding (*open circles*) and specific binding (*closed circles*). (*Bottom*) Scatchard analysis: correlation coefficient = 0.98; -1/slope = K_d = 0.4 μM.

As a second measure of binding, increasing amounts of labeled $T11_{ex2}$ were added to a constant number of JY cells. As shown in Fig. 6 (*top*), specific binding is saturable. These saturation binding data were transformed by Scatchard analysis (Fig. 6, *bottom*). Specific $T11_{ex2}$ binding is saturated at $\sim 300 \times 10^3$ molecules per cell. The Scatchard plot yields an estimated dissociation constant of 0.4 μM for the $T11_{ex2}$-LFA-3 interaction. Note that although a single incubation period (1 h at 4°C) of cells with ligand was used in these experiments, kinetic analysis demonstrates that maximal $T11_{ex2}$-LFA-3 binding occurs within 5 min.

Discussion

We have shown that a soluble, monomeric extracellular segment CD2 molecule, termed $T11_{ex2}$, carries epitopes recognized by antibodies against the native surface CD2 structure on resting T lymphocytes and interacts specifically with the surface-bound CD2 ligand LFA-3. The measured dissociation constant for this interaction is 0.4 μM, implying a low affinity relative to hormone receptor-ligand interactions (i.e., for IL-2 $K_d = 10^{-11}$ M) (23) but equivalent to that of primary antibody responses ($K_d = 10^{-5}$ to 10^{-6}) (30). The $T11_{ex2}$ molecule gives rise to a proteolytically resistant 15-kD NH_2-terminal papain fragment, suggesting that the NH_2-terminal ~100 amino acid residues comprise a stable, well-folded domain corresponding to a polypeptide encoded by the first extracellular exon. In contrast, despite disulfide linkages, the COOH-terminal-encoded extracellular domain is labile to papain.

Binding of Monomeric $T11_{ex2}$ Is Less Avid than that of Detergent-solubilized CD2. The dissociation constant presented here for the monomeric $T11_{ex2}$ molecule contrasts with the value of 50 nM reported for similar analyses on JY cells with a detergent-solubilized full-length CD2 molecule purified from T cells (9). In both cases the estimate of binding affinity derived by Scatchard analysis agrees quite well with that obtained by inhibition with unlabeled ligand. The two distinct interactions measured likely display real affinity differences. In addition, blocking estimates of the affinity of $T11_{ex2}$ for its ligand by rosette inhibition, blocking of anti-LFA-3 antibody binding, either of two distinct radiolabeled binding assays and preliminary studies of $T11_{ex2}$-mediated inhibition of clonal T cell proliferation (data not shown) all give results in the same range, i.e., a distinctly lower affinity that that reported for detergent-solubilized CD2.

Several possibilities may explain the difference in reported binding affinities. First, the presence of the hydrophobic transmembrane segment in the purified CD2 molecule may endow it with a different binding behavior than the membrane-anchorless $T11_{ex2}$ protein. For example, it is possible that interaction of the transmembrane segment with the cell membrane affects the maximal affinity. Second, detergent-solubilized CD2 probably exists as detergent/protein micelles, which might allow for a multivalent attachment of micelles to JY cells that could affect the observed dissociation constant: Such multipoint attachment would not be possible for the monomeric $T11_{ex2}$. However, one cannot rule out the possibility that $T11_{ex2}$ fails to adopt a conformation sufficiently like that of the native CD2 molecule to allow it to bind in a similar way. This might result from the absence of contributions from the transmembrane or cytoplasmic domains or differences in post-translational processing by SF9 cells as compared with human T lymphocytes. This possibility is made less likely by the fact that $T11_{ex2}$ carries epitopes for anti-CD2 antibodies that inhibit CD2-LFA-3 interaction and the unrelated $T11_2$ and $T11_3$ epitopes and by the fact that SF9 cells correctly cleave the CD2 signal peptide.

The relatively low affinity of $T11_{ex2}$ for LFA-3 needs to be viewed in the context of the cell biology of this ligand-receptor pair in cell-cell interactions. Clearly, CD2 does not exist as a soluble monomer on T cells, but rather as an array of cell-bound transmembrane structures consisting of multiple copies per cell, ranging from 20,000 on resting peripheral blood lymphocytes to 200,000 on activated T cells (13). Thus, a high affinity interaction between one CD2 and one LFA-3 molecule may not be required for a single binding event. Rather, a series of low affinity binding events

could be sufficient for two cells to adhere to one another by a multimeric interaction that would greatly enhance the avidity of the T cell for its cognate partner. Antigen-stimulated T cells express an order of magnitude more of surface CD2, perhaps in order to adhere better to presenting cells in areas of ongoing immune responses.

Substantial indirect evidence exists to suggest that the CD4 molecules on helper T cells and class II-restricted cytolytic T cells interact with class II MHC molecules on stimulator or target cells (31–33). Abrogation of this interaction by anti-CD4 or anti-class II antibodies profoundly influences T cell responses. The inability to observe a direct physical interaction between CD4 and Ia and to inhibit cellular interactions with micromolar amounts of soluble CD4 (19) suggests that low affinity interactions are of fundamental significance for physiologic T cell function.

The Relationship of CD2 to the Ig Superfamily. Several reports argue for the inclusion of CD2 in the Ig superfamily (26, 34, 35). The defining characteristic of members of this family is the presence of one or more Ig folds that comprise two β-sheets, each containing three or four antiparallel β-strands, 5–10 amino acids in length. Nearly all Ig folds contain an intrachain disulfide link. The fold is markedly resistant to proteolysis which may reflect the need for Ig-like molecules to retain function in extracellular spaces where they may be exposed to proteases. Immune system molecules predicted to have at least one such domain include the MHC antigens, CD4 and CD8 structures, Thy-1 molecule, and poly-Ig receptor. A variety of cell surface molecules found on cells outside the immune system have also been suggested to belong to this family, including the NCAM and ICAM-1 cell adhesion molecules and platelet-derived growth factor and CSF-1 receptors (reviewed in reference 26).

The exon-intron organization of CD2 divides its external segment into two domains: I, amino acids 1–103; and II, amino acids 104–180. Consistent with this division, limited papain digestion of soluble CD2 molecule $T11_{ex2}$ clearly demonstrates the existence of a stable NH_2-terminal fragment of ~100 residues. Both domains I and II have been suggested to adopt Ig structures on the basis of primary sequence homology with other Ig family members (26).

Although the alignment scores for these domains are statistically significant when tested against other members of the Ig superfamily, certain difficulties are apparent. If both CD2 domains are Ig-like, the extracellular domain should not contain any α-helical structure. However, earlier secondary structural predictions suggest the presence of α-helices, with a particularly strong prediction for the NH_2-terminal 10–20 residues (16). In addition, circular dichroism data for the $T11_{ex2}$ molecule, which includes both domains, predict substantial (~20%) α-structure when analyzed by either of two deconvolution methods. If this interpretation of the CD profile is correct, and if $T11_{ex2}$ adopts a configuration similar to native CD2, as is suggested by its ability to be recognized by anti-CD2 antibodies and to bind specifically to a cell-surface ligand for CD2, LFA-3, it would appear unlikely that both CD2 domains adopt Ig folds.

Given that the 15-kD domain I fragment can be obtained in high yield from the soluble CD2 molecule described here, it should be informative to analyze the fragment alone by circular dichroism. Apparently, it also folds correctly since it can be recognized by anti-$T11_1$ and anti-$T11_2$ antibodies and inhibits sheep erythrocyte rosetting to T cells (24). If the secondary structure predictions (16) are correct, this analysis should reveal a mix of α-helical and β-sheet structures. The availability of

both the entire extracellular segment and the fragment in large amounts could also allow for crystallographic analysis.

The present report has emphasized the role of the CD2 external segment in facilitating T lineage–specific cell adhesion. Clearly, this CD2-dependent process is critical for physiologic T cell function and thymocyte-thymic epithelial cell interaction. Given the lineage-restricted nature of the CD2 adhesion molecule and the high level of LFA-3 expression on thymic epithelial cells (5), it is quite likely that CD2 plays a major role in intrathymic differentiation.

Summary

The 50-kD CD2 (T11) surface glycoprotein on human T lymphocytes and thymocytes plays a critical role in T lineage cell activation and adhesion via its ligand LFA-3. To begin to define structure-function relationships in the extracellular segment of the transmembrane CD2 molecule, we have used a eukaryotic expression system and a CD2 cDNA to produce milligram amounts of recombinant soluble CD2 molecule that corresponds to the two extracellular segment exons. We show that this protein, termed $T11_{ex2}$, behaves as a monomer in aqueous solution and includes a proteolytically resistant NH_2-terminal fragment (domain I) encoded by the first extracellular segment exon. Circular dichroism analysis of $T11_{ex2}$ demonstrates that its stabilized secondary structure is dependent on the intrachain disulfide bonds present in domain II. The $T11_{ex2}$ monomer binds directly to the CD2 ligand LFA-3 with a dissociation constant of 0.4 μM. This relatively low affinity implies that cooperative binding resulting from an array of transmembrane CD2 molecules is important to facilitate physiologic T cell adhesion.

We thank Drs. Kendall Smith for helpful discussions regarding binding analyses and Gerald Fasman regarding circular dichroism. We also acknowledge the excellent technical assistance of Neville Buttress, Amita Vaid, Yasmin Husain, and Ruth Steinbrich.

Received for publication 4 October 1988 and in revised form 1 December 1988.

References

1. Meuer, S. C., R. E. Hussey, M. Fabbi, D. Fox, O. Acuto, K. A. Fitzgerald, J. C. Hodgdon, J. P. Protentis, S. F. Schlossman, and E. L. Reinherz. 1984. An alternative pathway of T-cell activation: a functional role for the 50 kd T11 sheep erythrocyte receptor protein. *Cell.* 36:897.
2. Brottier, P., L. Boumsell, C. Gelin, and A. Bernard. 1985. T cell activation via CD2 [T, gp50] molecules: accessory cells are required to trigger T cell activation via CD2-D66 plus CD2-9.6/T11$_1$ epitopes. *J. Immunol.* 135:1624.
3. Siliciano, R. F., J. C. Pratt, R. E. Schmidt, J. Ritz, and E. L. Reinherz. 1985. Activation of cytolytic T lymphocyte and natural killer cell function through the T11 sheep erythrocyte binding protein. *Nature (Lond.).* 317:428.
4. Fox, D. A., R. E. Hussey, K. A. Fitzgerald, A. Bensussan, J. F. Daley, S. F. Schlossman, and E. L. Reinherz. 1985. Activation of human thymocytes via the 50kd T11 sheep erythrocyte binding protein induces the expression of interleukin 2 receptors on both $T3^+$ and $T3^-$ populations. *J. Immunol.* 134:330.
5. Denning, S. M., D. T. Tuck, L. W. Vollger, T. A. Springer, K. H. Singer, and B. F. Haynes. 1987. Monoclonal antibodies to CD2 and lymphocyte function-associated an-

tigen 3 inhibit human thymic epithelial cell-dependent mature thymocyte activation. *J. Immunol.* 139:2573.

6. Hunig, T. 1985. The cell surface molecule recognized by the erythrocyte receptor of T lymphocytes. *J. Exp. Med.* 162:890.
7. Hunig, T., G. Tiefenthaler, K. H. Meyer zum Buschenfelde, and S. C. Meuer. 1987. Alternative pathway activation of T cells by binding of CD2 to its cell-surface ligand. *Nature (Lond.).* 326:298.
8. Shaw, S., G. E. Ginther-Luce, R. Quinones, R. E. Gress, T. A. Springer, and M. E. Sanders. 1986. Two antigen-independent pathways used by human cytotoxic T-cell clones. *Nature (Lond.).* 323:262.
9. Selvaraj, P., M. L. Plunkett, M. Dustin, M. E. Sanders, S. Shaw, and T. A. Springer. 1987. The T lymphocyte glycoprotein CD2 binds the cell surface ligand LFA-3. *Nature (Lond.).* 326:400.
10. Vollger, L. W., D. T. Tuck, T. A. Springer, B. F. Haynes, and K. H. Singer. 1987. Thymocyte binding to human thymic epithelial cells is inhibited by monoclonal antibodies to CD-2 and LFA-3 antigens. *J. Immunol.* 138:358.
11. Howard, F. D., J. A. Ledbetter, J. Wong, C. P. Bieber, E. B. Stinson, and L. A. Herzenberg. 1981. A human T lymphocyte differentiation marker defined by monoclonal antibodies that block E-rosette formation. *J. Immunol.* 126:2117.
12. Brown, M. H., W. A. Sewell, E. Monostori, and M. J. Crumpton. 1987. Characterization of T cell epitopes by Western blotting. *In* Leucocyte Typing III. A. J. McMichael, editor. Oxford University Press, Oxford. 110–112.
13. Sayre, P. H., H. C. Chang, R. E. Hussey, N. R. Brown, N. E. Richardson, G. Spagnoli, L. K. Clayton, and E. L. Reinherz. 1987. Molecular cloning and expression of T11 cDNAs reveal a receptor-like structure on human T lymphocytes. *Proc. Natl. Acad. Sci. USA.* 84:2941.
14. Sewell, W. A., M. H. Brown, J. Dunne, M. J. Owen, and M. J. Crumpton. 1986. Molecular cloning of the human T-lymphocyte surface CD2 (T11) antigen. *Proc. Natl. Acad. Sci. USA.* 83:8718.
15. Seed, B., and A. Aruffo. 1987. Molecular cloning of the CD2 antigen, the T-cell erythrocyte receptor, by a rapid immunoselection procedure. *Proc. Natl. Acad. Sci. USA.* 84:3365.
16. Clayton, L. K., P. H. Sayre, J. Novotny, and E. L. Reinherz. 1987. Murine and human T11 (CD2) cDNA sequences suggest a common signal transduction mechanism. *Eur. J. Immunol.* 17:1367.
17. Diamond, D. J., L. K. Clayton, P. H. Sayre, and E. L. Reinherz. 1988. Exon-intron organization and sequence comparison of human and murine T11 (CD2) genes. *Proc. Natl. Acad. Sci. USA.* 85:1615.
18. Smith, G. E., G. Ju, B. L. Ericson, J. Moschera, H. W. Lahm, R. Chizzonite, and M. D. Summers. 1985. Modification and secretion of human interleukin 2 produced in insect cells by a baculovirus expression vector. *Proc. Natl. Acad. Sci. USA.* 82:8404.
19. Hussey, R. E., N. E. Richardson, M. Kowalski, N. R. Brown, H. C. Chang, R. F. Siliciano, T. Dorfman, B. Walker, J. Sodroski, and E. L. Reinherz. 1988. A soluble CD4 protein selectively inhibits HIV replication and syncytium formation. *Nature (Lond.).* 331:78.
20. Matsudaira, P. 1987. Sequence from picomole quantities of proteins electroblotted onto polyvinylidene difluoride membranes. *J. Biol. Chem.* 262:10035.
21. Yphantis, D. A. 1964. Equilibrium sedimentation of dilute solutions. *Biochemistry.* 3:297.
22. Richardson, N. E., N. Buttress, A. Feinstein, A. Stratil, and R. L. Spooner. 1973. Structural studies on individual components on bovine transferrin. *Biochem. J.* 135:87.
23. Teshigawara, K., H-M. Wang, K. Kato, and K. A. Smith. 1987. Interleukin 2 high affinity receptor expression depends on two distinct binding proteins. *J. Exp. Med.* 165:223.
24. Richardson, N. E., H. C. Chang, N. R. Brown, R. E. Hussey, P. H. Sayre, and E. L.

Reinherz. 1988. The adhesion domain of human T11 (CD2) is encoded by a single exon. *Proc. Natl. Acad. Sci. USA.* 85:5176.

25. Campbell, D. G., A. F. Williams, P. M. Bayley, and K. B. M. Reid. 1979. Structural similarities between Thy-1 antigen from rat brain and immunoglobulin. *Nature (Lond.).* 282:341.
26. Williams, A. F., and A. N. Barclay. 1988. The immunoglobulin superfamily domains for cell surface recognition. *Annu. Rev. Immunol.* 6:381.
27. Compton, L. A., and W. C. Johnson. 1986. Analysis of protein circular dichroism spectra for secondary structure using a simple matrix multiplication. *Anal. Biochem.* 155:155.
28. Yang, J. T., C. S. C. Wu, and H. M. Martinez. 1986. Calculation of protein conformation from circular dichroism. *Methods. Enzymol.* 130:208.
29. Sanchez-Madrid, F., A. Krensky, C. F. Ware, E. Robbins, J. L. Strominger, S. J. Burakoff, and T. A. Springer. 1982. Three distinct antigens associated with human T-lymphocyte-mediated cytolysis: LFA-1, LFA-2, and LFA-3. *Proc. Natl. Acad. Sci. USA.* 79:7489.
30. Eisen, H. W., and G. W. Siskind. 1964. Variations in affinities of antibodies during the immune response. *Biochemistry.* 3:996.
31. Meuer, S. C., S. F. Schlossman, and E. L. Reinherz. 1982. Clonal analysis of human cytotoxic T lymphocytes: $T4^+$ and $T8^+$ effector T cells recognize products of different major histocompatibility complex regions. *Proc. Natl. Acad. Sci. USA.* 79:4395.
32. Krensky, A. M., C. Clayberger, C. S. Reiss, J. L. Strominger, and S. J. Burakoff. 1982. Specificity of $OKT4^+$ cytotoxic T lymphocyte clones. *J. Immunol.* 129:2001.
33. Doyle, C., and J. L. Strominger. 1987. Interaction between CD4 and class II MHC molecules mediates cell adhesion. *Nature (Lond.).* 330:256.
34. Williams, A. F., A. N. Barclay, S. J. Clark, D. J. Patterson, and A. C. Willis. 1987. Similarities in sequences and cellular expression between rat CD2 and CD4 antigens. *J. Exp. Med.* 165:368.
35. Peterson, A., and B. Seed. 1987. Monoclonal antibody and ligand binding sites of the T cell erythrocyte receptor (CD2). *Nature (Lond.).* 329:842.